






Article

Generation of Cobalt-Containing Nanoparticles on Carbon via Pyrolysis of a Cobalt Corrole and Its Application in the Hydrogenation of Nitroarenes

Jessica Michalke ¹, Michael Haas ², Dominik Krisch ², Thomas Bögl ³ , Stephan Bartling ⁴ , Nils Rockstroh ⁴ , Wolfgang Schöfberger ²  and Christoph Topf ^{1,*} 

¹ Institute of Catalysis (INCA), Johannes Kepler University (JKU), Altenberger Straße 69, 4040 Linz, Austria; jessica.michalke@jku.at

² Institute of Organic Chemistry, Johannes Kepler University (JKU), Altenberger Straße 69, 4040 Linz, Austria; michael.haas@jku.at (M.H.); dominik.krisch@jku.at (D.K.); wolfgang.schoefberger@jku.at (W.S.)

³ Department of Analytical Chemistry, Johannes Kepler University (JKU), Altenberger Straße 69, 4040 Linz, Austria; thomas.boegl@jku.at

⁴ Leibniz Institute for Catalysis e. V. (LIKAT Rostock), Albert-Einstein-Straße 29a, 18059 Rostock, Germany; stephan.bartling@catalysis.de (S.B.); nils.rockstroh@catalysis.de (N.R.)

* Correspondence: christoph.topf@jku.at

Abstract: We report on the manufacture of a state-of-the-art heterogeneous non-noble metal catalyst, which is based on a molecularly well-defined phosphine-tagged cobalt corrole complex. This precursor compound is readily synthesized from convenient starting materials while the active material is obtained through wet-impregnation of the pertinent metalliferous macrocycle onto carbon black followed by controlled pyrolysis of the loaded carrier material under an inert gas atmosphere. Thus, the obtained composite was then applied in the heterogeneous hydrogenation of various nitroarenes to yield a vast array of valuable aniline derivatives that were conveniently isolated as their hydrochloride salts. The introduced catalytic protocol is robust and user-friendly with the entire assembly of the reaction set-up enabling the conduction of the experiments on the laboratory bench without any protection from air.

Keywords: base metal catalysis; heterogeneous hydrogenation; cobalt; corrole; pyrolysis



Citation: Michalke, J.; Haas, M.; Krisch, D.; Bögl, T.; Bartling, S.; Rockstroh, N.; Schöfberger, W.; Topf, C. Generation of Cobalt-Containing Nanoparticles on Carbon via Pyrolysis of a Cobalt Corrole and Its Application in the Hydrogenation of Nitroarenes. *Catalysts* **2022**, *12*, 11. <https://doi.org/10.3390/catal12010011>

Academic Editor: Ken-ichi Fujita

Received: 24 November 2021

Accepted: 20 December 2021

Published: 23 December 2021

Publisher's Note: MDPI stays neutral with regard to jurisdictional claims in published maps and institutional affiliations.



Copyright: © 2021 by the authors. Licensee MDPI, Basel, Switzerland. This article is an open access article distributed under the terms and conditions of the Creative Commons Attribution (CC BY) license (<https://creativecommons.org/licenses/by/4.0/>).

1. Introduction

The synthesis of aniline from nitroarenes is a highly relevant industrial process considering the high demand of aromatic amines for the production of pharmaceuticals, dyestuffs, agrochemicals, and isocyanates for making polyurethanes. Traditionally, the given nitro reduction is realized through the stoichiometric Béchamp reaction, which deploys highly corrosive hydrochloric acid and excess iron powder [1]. Since this route produces a significant amount of inorganic waste, it is worthwhile, for both economic and ecological reasons, to resort to catalytic methods utilizing H₂ gas as the principal reductant. In this case, the pertinent chemical transformation is rendered more cost- and atom-efficient, given the low price of hydrogen and the fact that only water is formed as the by-product [2–5].

Concerning homogeneous approaches, the published procedures report the use of precious metals such as Au [6], Ir [7], Pd [8,9], Pt [10], Rh [11], or Ru [12–14], whereas non-noble, metal-based strategies center around the implementation of Fe [12,15,16], Mn [17], or Co [18] as catalytically active metal centers in the complexes that mediate the desired reaction.

Regarding heterogeneous catalysis, the first reports by Beller and coworkers dealing with the title reaction brought about by carbonaceous N-doped catalysts accessible through pyrolytic syntheses from suitable metal-ligand assemblies [19–21] have significantly forwarded the field of heterogeneous base-metal redox catalysis. Expanding upon these seminal works, an impressive number of reports dealing with both the manufacture of

related cobalt-containing hybrid materials and their application in the nitroarene reduction, either relying on gaseous H_2 or selected transfer reagents (hydrazine, formic acid), has appeared in recent years [22–45]. With respect to the catalyst performance of such supported heteroatom-doped solids, it was borne out through experiments that the activity is directly proportional to the *N*-content of the composite that brings about the desired transformation [46]. Consequently, the use of nitrogen-rich (chelating) *N*-donor ligands is an effective tool for the preparation of decent heterogeneous catalysts that are activated through controlled thermal heat treatment of a molecularly well-defined metal complex.

In addition to the above-mentioned strategy, pyrolysis-free approaches relying on cobalt are also well-documented in pertinent literature protocols, and a variety of Co-based solids have been demonstrated to effectively drive the hydrogenation of nitroarenes [47–52]. Finally, the highly reactive but pyrophoric and nonselective Raney[®] Ni, as well as the expensive Pd-on-charcoal, can also be used for the reduction of aromatic nitro compounds to afford anilines [3].

Notwithstanding the great success of composites that are based on certain annealed coordination compounds, their manufacture entails a time-consuming complexation step that is carried out in solution prior to wet-impregnation of the support. Thus, it seemed worthwhile to employ a prefabricated (and, ideally, commercially available) complex that already incorporates the catalytically active metal and a nitrogen-rich ligand to guarantee good performance. In this regard, cost-effective cyanocobalamin (vitamin B₁₂, Figure 1a) represents a sound choice, and specific materials derived therefrom have found promising applications as catalysts in fuel cells [53], in the oxygen reduction-reaction (ORR) [54], and in the hydrogen evolution reaction (HER) [55]. Furthermore, in the context of organic synthesis, mesoporous carbon prepared from this coenzyme was shown to foster the formation of imines that constitute vital intermediates in the production of pharmaceuticals [56]. In addition, ceria-supported and pyrolytically-activated cyanocobalamin was employed in the heterogeneous hydrogenation of nitrile derivatives to afford valuable benzylamines (Figure 1a) [57].

Although pristine cobalt-based cobalamins indeed serve as reasonable (solution phase) precursors for the fabrication of heterogenized catalysts, their thermal heat treatment entails the inevitable annihilation of precious stereocenters that are located in the pendent sidechains of the molecules. Hence, the overall pyrolysis processes conducted with such biomolecules suffer from very low atom efficiencies. As a consequence of this, the development of more rational production methods for related solid composite materials is highly sought after.

Guided by the very close structural resemblance of the vitamin B₁₂ core structure (corrin, Figure 1b) and the corrole framework (Figure 1c), as well as the facile synthetic access to the latter, we decided to test the suitability of this porphyrin-related macrocycle class as a source for the manufacture of pyrolysis-based heterogeneous non-noble metal catalysts.

In general, the syntheses and in-depth characterization of corroles, including their metalliferous congeners—especially those containing cobalt—constitutes a well-established body of science [58–63], and certain metal corrole complexes were previously successfully applied for the design of catalysts applicable for water splitting [64], redox-transformations involving gaseous O_2 [65–67], and CO_2 electroreduction [68,69]. Quite recently, with respect to molecular catalysis, a DMSO-tagged cobalt-corrole complex was demonstrated to affect the title transformation (Figure 2a) [18]. Lastly, related Co-corrolates were developed into sensors suitable for the detection of CO gas [70], as well as ions such as nitrite and nitrate ions [71,72].

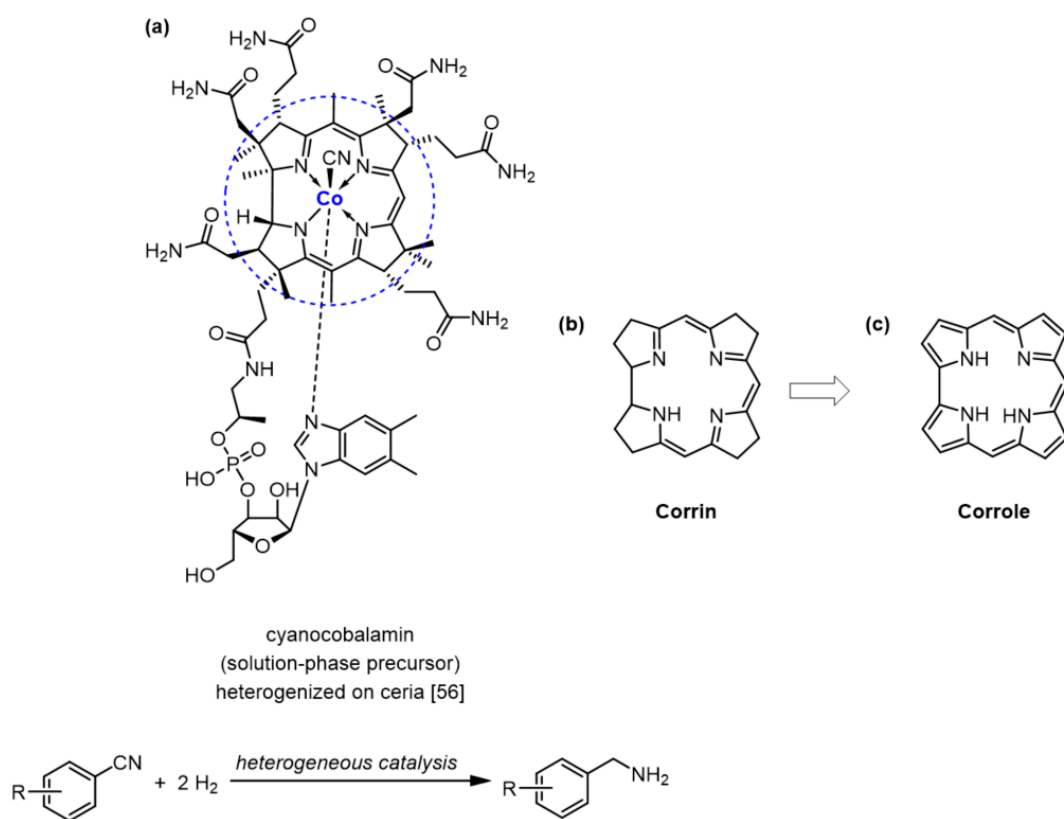
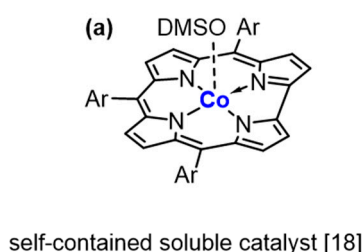


Figure 1. (a) Naturally occurring vitamin B₁₂ (cyanocobalamin) has previously been applied as a precursor compound for the preparation of a solid ceria-supported catalyst that facilitated the pressure hydrogenation of benzonitrile derivatives. (b) Structural drawing of the corrin base frame upon which vitamin B₁₂ and kindred bioactive macrocyclic metal complexes are built upon. (c) Molecular structure of the corrole scaffold that herein serves as the key motif for the design of a carbonaceous N-doped heterogeneous hydrogenation catalyst based on cobalt.

Previous work:



This work:

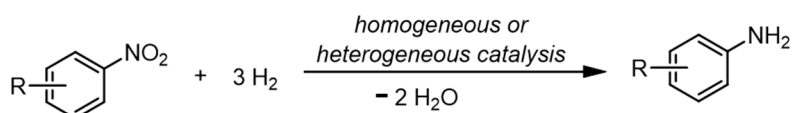
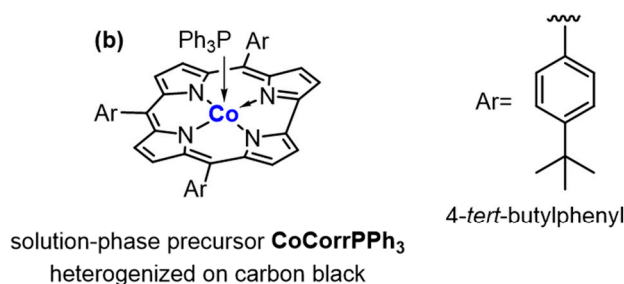


Figure 2. (a) A molecularly well-defined cobalt-corrole complex was shown to bring about the homogeneous hydrogenation of nitroarenes to afford a variety of aniline derivatives [18]. (b) Herein, a pre-fabricated phosphine-tagged cobalt corrole, which can be considered as a curtailed vitamin B₁₂ analog, was merged with carbon black (Vulcan[®] XC 72 R) and then pyrolytically activated to catalyze the same nitroarene-to-aniline hydrogenation.

Apart from the favorable *N*-content of the bare corrole backbone (*vide supra*), the architecture of the entire Co-corrole assembly allows for the accommodation of an additional axial ligand that incorporates heteroatoms other than nitrogen (Figure 2b). This feature, in turn, offers the intriguing possibility of specifically co-doping the full-fledged catalyst at the early easy-to-modify molecular level. In this respect, special emphasis is placed on phosphorus since this element is well known to ameliorate the redox activity (including the hydrogenation activity) of the respective catalysts [73–92].

Herein, we introduce the fabrication of a solid, carbon black-supported *N*, and a *P* co-doped catalyst that was prepared from a triphenylphosphine-ligated cobalt corrole through controlled pyrolysis in an argon atmosphere. Thus, the prepared composite was then utilized in the highly relevant heterogeneous pressure hydrogenation of nitroarenes to yield the corresponding aniline derivatives, which were readily precipitated from the filtered reaction solution as their hydrochlorides (*vide infra*).

2. Results and Discussion

2.1. Catalyst Preparation and Characterization

Imbuing a commercial Vulcan® XC 72 R powder with an ethanolic solution of pre-synthesized CoCorrPPh₃ (see Figure 2 for the structural drawing), subsequent removal of the volatiles under reduced pressure, and the ensuing annealing of the modified support at 800 °C under an inert gas atmosphere (argon) furnished the catalytically active compound CoCorrPPh₃@Vulcan-800. The experimental details for the manufacture of this heterogeneous catalyst are outlined in Section 3.1.

In order to obtain qualitative information about the surface composition of the pyrolytically synthesized cobalt catalyst, we employed the use of XPS. Deconvolution of the pertinent N 1s spectrum (Figure 3) exposed three individual peaks that are ascribed to pyridinic-, pyrrolic-, and graphitic-type nitrogen (with the intensity of the respective signals decreasing in the order listed). Owing to the partial overlap of the spectroscopic features, it was not possible to unequivocally quantify the single contributions of the three N species to the total nitrogen content. Notwithstanding this fact, the results of the XPS analysis proved that nitrogen is indeed incorporated into the Vulcan® matrix upon thermally induced conversion of the corrole framework.

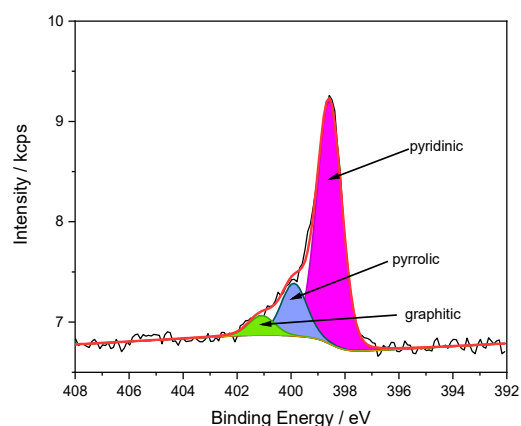


Figure 3. High-resolution N 1s spectra (XPS) of the pyrolytically-activated CoCorrPPh₃@Vulcan-800 catalyst showing three different nitrogen modifications, i.e., pyridinic (major share), pyrrolic (medium share), and graphitic (minor share); the total (surface) N content amounted to 1.3 atom-%.

The full range of the recorded X-ray photoelectron spectrum as well as an enlarged portion displaying the cobalt-related region are depicted in Figure S1 and Figure S2, respectively (see Supplementary Materials).

High-angle annular dark-field scanning transmission electron microscopy (HAADF-STEM) was used to gain deeper insight into the morphology of CoCorrPPh₃@Vulcan-800 (Figure 4). The images reveal relatively large cobalt-based particles that are widely

distributed over the surface of the Vulcan[®] carrier material. Furthermore, the composition of these particles is not uniform, which is, for instance, indicated in Figure 4c.

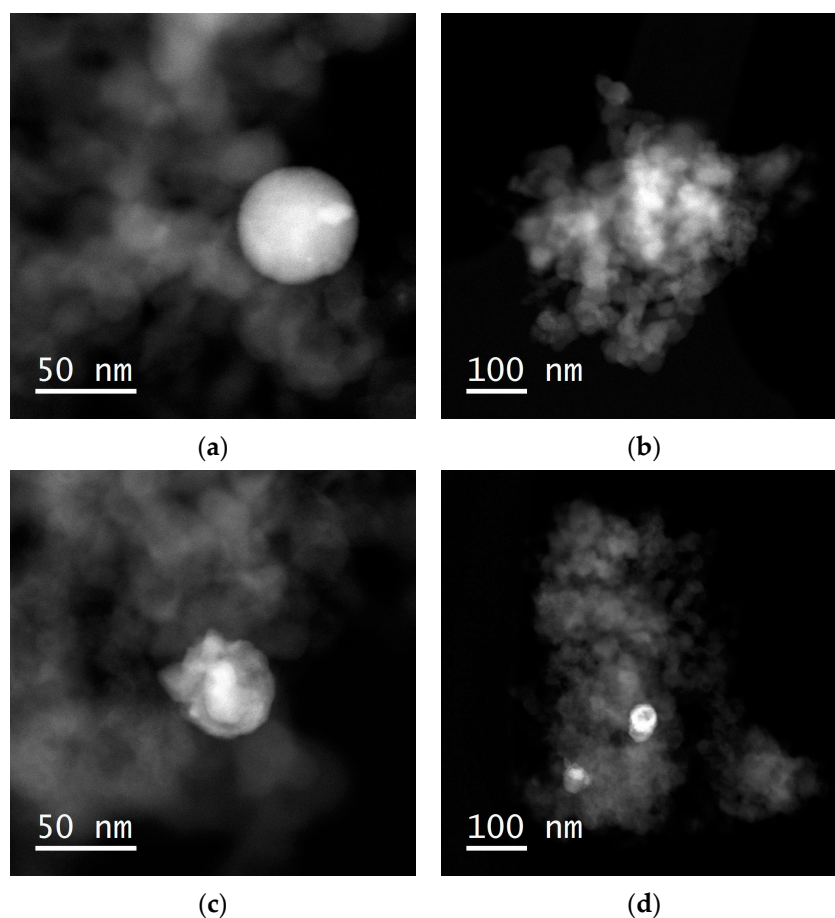


Figure 4. (a–d). Selected HAADF-STEM images of the catalytically active composite CoCorrPPh₃@Vulcan-800.

Energy-Dispersive X-ray Spectroscopy (EDX) was deployed to establish both the chemical constitution and the architecture of the metalliferous particles. Upon evaluation of the EDX spectra, we infer that there are cobalt containing particles being composed of a cobalt phosphide core that is surrounded by a cobalt oxide shell (Figure S3).

2.2. Catalytic Tests

To assess the catalytic performance of the heterogenized cobalt corrolate in the hydrogenation of nitrobenzene (Figure 5), we applied free, thermally decomposed CoCorrPPh₃ as well as Vulcan[®]-, ceria-, silica-, and alumina-supported modifications thereof (Table 1). The solely heat-treated metal complex already gave rise to a 60% substrate conversion (Entry 5), whereas attaching the pyrolyzed metal corrole assembly onto the Vulcan[®] powder improved this value by almost 20% (Entry 1). The other investigated carrier materials, i.e., CeO₂, SiO₂, and Al₂O₃, were all heavily outperformed by the canonical Vulcan[®] XC 72 R (3–26% conversion of nitrobenzene, Entries 2–4).

Of note, the pristine and non-pyrolyzed solution phase precursor CoCorrPPh₃ represents a hydrogenation catalyst on its own that facilitates the given nitrobenzene-to-aniline reduction to a provable extent (Entry 6) [18]. Quite remarkably, the activity of the phosphine-ligated cobalt corrole ceases on mere immobilization on Vulcan[®] without subsequent pyrolysis of the impregnated material (Entry 7).

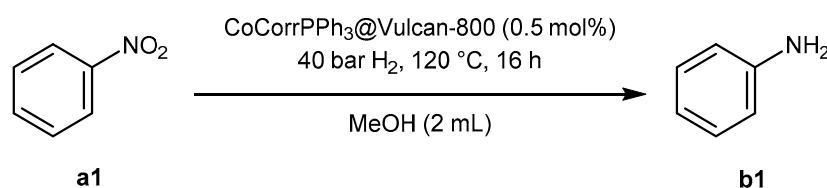


Figure 5. Model hydrogenation of nitrobenzene to aniline effected by CoCorrPPh₃@Vulcan.

Table 1. Dependence of the catalyst activity on the chemical nature of the support. Reaction conditions: nitrobenzene (0.25 mmol), catalyst (0.5 mol%), H₂ (40 bar), MeOH (2 mL), 120 °C, 16 h, and *n*-hexadecane as an internal standard (18 mg). The indication of the catalyst quantity is based on the bulk metal content as determined by the elemental analysis.

Entry	Catalyst	Pyrolysis T (°C)	Conversion (%)
1	CoCorrPPh ₃ @Vulcan	800	79
2	CoCorrPPh ₃ @CeO ₂	800	26
3	CoCorrPPh ₃ @SiO ₂	800	7
4	CoCorrPPh ₃ @Al ₂ O ₃	800	3
5	CoCorrPPh ₃	800	60
6	CoCorrPPh ₃	non-pyrolyzed	7
7	CoCorrPPh ₃ @Vulcan	non-pyrolyzed	0

Having identified the ideal support for the given cobalt-catalyzed nitrobenzene hydrogenation, we investigated the influence of the catalyst amount on the substrate conversion (Table 2). Using loadings as low as 0.10 mol% and 0.25 mol% still enabled detectable conversions of 9% and 25%, respectively (Entries 1 and 2), while increasing the portion to 0.5 mol% allowed for a decent 79% (Entry 3). Finally, application of 1 mol% of CoCorrPPh₃@Vulcan-800 completely converted the NO₂ motif in the model compound **a1** (Entry 4). Rewardingly, we established that a proper catalyst amount of 0.5 mol% per nitro group generally suffices for decent product formation (*vide infra*).

Table 2. Influence of the catalyst amount on the nitrobenzene-to-aniline hydrogenation. Reaction conditions: nitrobenzene (0.25 mmol), H₂ (40 bar), CoCorrPPh₃@Vulcan-800 catalyst, MeOH (2 mL), 120 °C, 16 h, and *n*-hexadecane as internal standard (18 mg).

Entry	Catalyst (mol%)	Conversion (%)
1	0.10	9
2	0.25	25
3	0.50	79
4	1.00	>99
5	no catalyst	0

Next, the effect of the pyrolysis temperature regarding the CoCorrPPh₃-impregnated Vulcan[®] carrier on the catalyst performance was probed (Table 3). We commenced with 400 °C, whereby an onset value of 22% conversion was observed. Upon constantly increasing the oven temperature, the catalyst activity successively increased to culminate with a 79% conversion at 800 °C (Entry 4). This result is well in line with the outcome of the Thermogravimetric Analysis (TGA) (Figure S4 in the supporting information part). Importantly, going beyond this temperature causes a steep decline of the nitrobenzene conversion by 25% (Entry 5); as expected, the non-pyrolyzed samples did not produce any aniline product (Entry 6).

Table 3. Hydrogenation of nitrobenzene; optimization of the pyrolysis temperature. Reaction conditions: nitrobenzene (0.25 mmol), CoCorrPPh₃@Vulcan-X (0.5 mol%), H₂ (40 bar), MeOH (2 mL), 120 °C, 16 h, and *n*-hexadecane as internal standard (18 mg). X denotes the pyrolysis temperature in °C.

Entry	Catalyst	Pyrolysis T (°C)	Conversion (%)
1	CoCorrPPh ₃ @Vulcan	400	22
2	CoCorrPPh ₃ @Vulcan	600	46
3	CoCorrPPh ₃ @Vulcan	700	69
4	CoCorrPPh ₃ @Vulcan	800	79
5	CoCorrPPh ₃ @Vulcan	900	54
6	CoCorrPPh ₃ @Vulcan	non-pyrolyzed	0

We then went on to study the impact of the reaction medium on the activity of the solid CoCorrPPh₃@Vulcan-800 composite catalyst (Table 4). The model reaction performs best in a protic polar media (Entries 1–3), whereas in the common THF the nitrobenzene conversion sharply dropped to a poor 14% (Entry 4); in nonpolar solvents (*n*-heptane, toluene) as well as in chloroform, the catalytic activity fully collapsed (Entries 5–7). Owing to the good solubility of anilinium chloride in water, the corresponding product yield was rather poor (55%) and hence, we decided to use methanol throughout this work as this solvent gave excellent results (Entry 2).

Table 4. Hydrogenation of nitrobenzene: optimization of the solvent. Reaction conditions: nitrobenzene (0.25 mmol), CoCorrPPh₃@Vulcan-800 (0.5 mol%), H₂ (40 bar), solvent (2 mL), 120 °C, 16 h, *n*-hexadecane as an internal standard (18 mg).

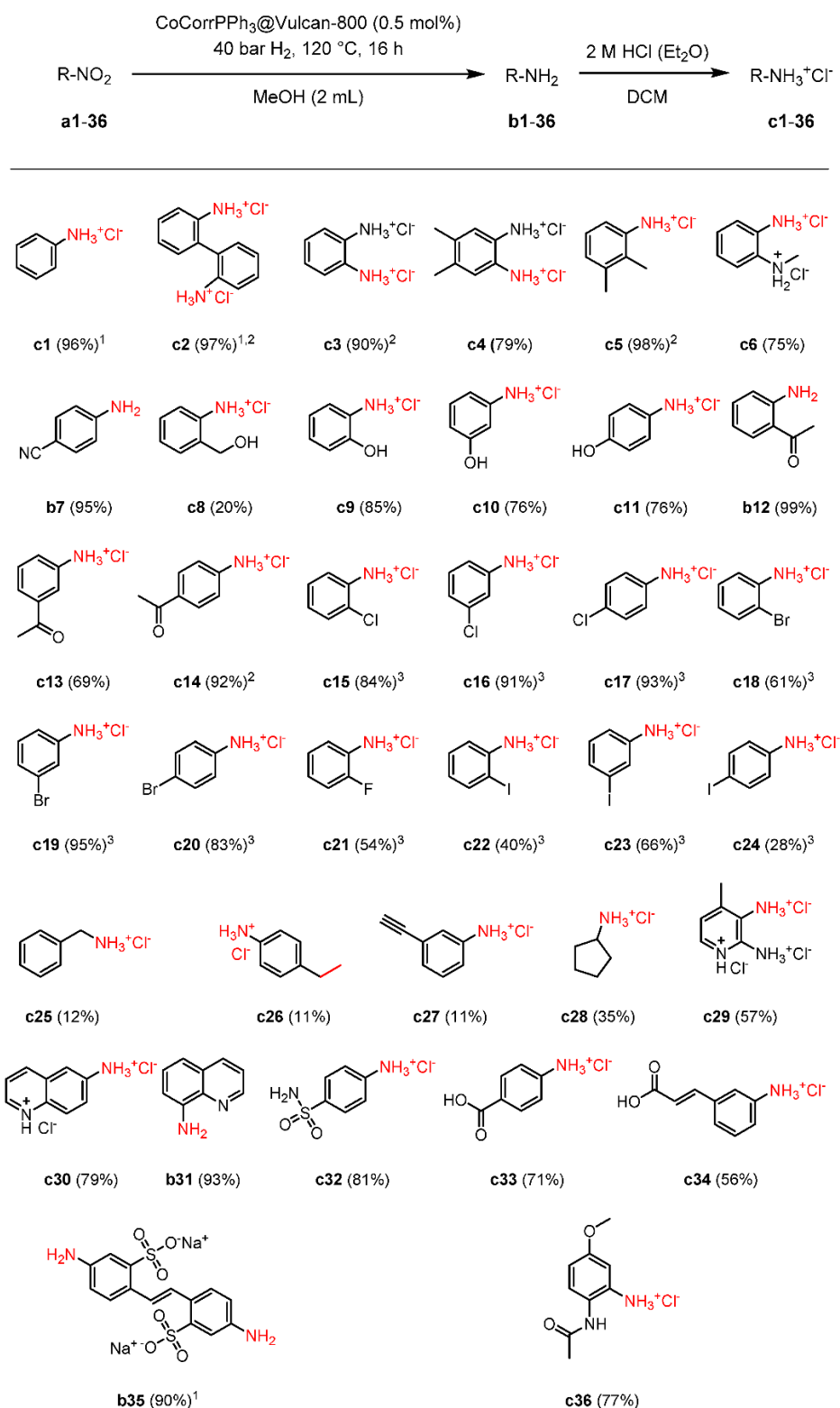
Entry	Solvent	Conversion (%)
1	MeOH	79
2	MeOH	>99 ¹ , (96) ¹
3	H ₂ O	>99 ¹ , (55) ¹
4	THF	14
5	<i>n</i> -heptane	0
6	toluene	0
7	CHCl ₃	0

¹ 1 mol% of catalyst was used, no internal standard was added, isolated yields of the corresponding hydrochloride salts are given in parentheses.

2.3. Scope and Limitations

After the systematic variation of the reaction parameters (*vide supra*), we intended for the elaboration of a general application protocol for the given heterogeneous cobalt catalyst (Scheme 1). The parent nitrobenzene **a1**, as well as its bis-congener **a2**, were neatly converted to afford the desired ammonium salts in an excellent yield (96% and 97%, respectively). However, placing the strong electron donating NH₂ functionality in direct proximity to the nitro motif (**a3**) slightly hampered the product formation (90%) that was exacerbated when two additional Me groups (**a4**) were present in the phenyl ring (79%). Yet, putting two small alkyl rests next to the nitro group (**a5**) re-established the almost quantitative formation of the desired anilinium derivative. Furthermore, we noticed that *N*-methylation of an adjacent amino group (**a6**) practically had the same effect in terms of product yield (75%) as if the arene ring had been alkylated twice (**a4**).

To our delight, the given heterogeneous catalyst system is tolerant of nitrile groups and, accordingly, the CN-tagged aniline **b7** was isolated in an excellent yield (95%). On the other hand, if an *ortho*-hydroxymethyl tether was located in the aryl moiety (**a8**) then the reaction outcome was inferior (20%). Strikingly, equipment of the phenyl ring with a pure OH group (**a9–a11**) in either position drastically increased the extent of product formation (76–85%).



Scheme 1. The complete scope of anilinium salts and free (heterocyclic) anilines that were made accessible through the CoCorrPPh₃@Vulcan-800-catalyzed heterogeneous hydrogenation of the respective nitroarenes. In one case, i.e., compound **c28**, a cycloaliphatic ammonium salt was produced. The percent value in parentheses refers to the isolated yield of the corresponding organic ammonium salt. ¹ The catalyst amount was doubled (1.0 mol%). ² The reaction time was 20 h. ³ The reaction time was reduced to 5 h.

An outstanding characteristic of the present pyrolytically-activated cobalt catalyst is its ability to sharply discriminate between the target NO₂ and a ketone motif. With an *o*- or *p*-acetyl group (**a12**, **a14**), nearly perfect chemoselectivity was observed (99% and 92% yield, respectively), though the same CH₃CO fragment in the *meta*-position provided only a mediocre formation of the wanted product, **c13** (69%).

With respect to the industrially relevant halide-functionalized substrates **a15**–**a24**, the best results were obtained with Cl- and Br-containing nitrobenzenes, particularly when the pertinent halogen atoms were fixed in the *meta*- or *para*-position (91% and 93% for the chloro-derivative, whereas 95% and 83% for the bromo-kindred); in the case of the *ortho*-congeners, the yields amounted to 84% for the Cl- and 61% for the Br-bearing substrate (**a15** and **a18**), respectively. [93] This markedly diminished product generation is likely to result from the steric hindrance that is imparted to the nitro group by the immediate vicinity of the respective halide substituent. Considering this detrimental size effect of the halogen atoms alone, it is, however, counterintuitive that the *o*-fluoro compound **a21** produced the required salt to an even lesser extent (54%). Given the fact that the F-atom is considerably smaller than its group, the VII homologs, the expected yield of salt **c21** is expected to be higher than (or at least the same as) 84%. Regarding the iodo-based substrates, the H₂-driven nitro-to-amine conversion severely suffered from hydro-dehalogenation and the outcome for the relevant position isomers **a22**–**a24** was moderate to poor (28–66%), with the *meta*-compound giving rise to the best result.

We then applied the given hydrogenation method to the CH₂-extended nitrobenzene **a25** and, surprisingly, the activity of the used solid cobalt catalyst nearly completely ceased (12% **c25**). This experimental finding highlights the necessity for a direct arene-NO₂ linkage to enable proper product formation. Furthermore, the presence of vinyl (**a26**) or alkynyl groups (**a27**) at the periphery of the used starting material proved to be deleterious for the amine formation too (11% yield in both cases). Compound **a27** with its C≡C bond was at least chemoselectively reduced and leaving the triple bond untouched, whereas both the **a26** nitro group and the C≡C motif were reduced. In addition to this, the alicyclic species **a28** and the multi-functionalized pyridine **a29** produced similar unsatisfactory results (35% and 57%, respectively).

Continuing with the *N*-heterocyclic substrates, we found that nitro-tagged quinolines **a30** and **a31** permitted legitimate reaction outcomes with the *peri*-substituted congener, giving rise to an even and very good yield of the free amine **b31**, which exceeded 90%. Moreover, the sulfonamide-based nitrobenzene **a32** is strongly compatible with the given hydrogenation protocol and the respective product was obtained in decent amounts (81%). To our delight, the solid CoCorrPPh₃@Vulcan-800 catalyst is reconciled with the presence of pendent carboxylic acids (substrates **a33** and **a34**), which are notoriously recalcitrant substrates for base metal-catalyzed hydrogenation reactions. Moreover, for substrate **a34**, the catalyst did not exhibit any activity towards the activated double bond.

One of the most important performance characteristics of our catalyst system is the provision of a brisk and atom-efficient route to disodium-4,4'-diamino-2,2'-stilbenedisulfonate **b35**, which is a key compound for the production of optical brighteners [94].

Finally, we found that this catalytic protocol also duly accommodates reducible amide bonds, as was proven upon application of a representative acetamido-tagged substrate (77% **c36**).

2.4. Recyclability Tests

For the reusability test of CoCorrPPh₃@Vulcan-800, we applied 4-nitrobenzonitrile as the model substrate to additionally verify whether the chemoselectivity of the transformation is retained upon performing the hydrogenation of the given starting material several times (nine runs) with one particular catalyst loading (Table 5). Upon finishing two cycles, the catalyst activity was still very good (Entries 1–2), whereas after the third iteration a marked decrease to 59% conversion was observed. After the fifth run, a value of 44% was observed, which remained, quite remarkably, almost constant until the end of the

series (Entries 5–9). Analyses of the reaction solutions revealed that in neither case was the nitrile motif reduced, and thus, the selectivity of the spent Co-catalyst was unaffected upon multiple uses.

Table 5. Recycling experiments for the liquid phase hydrogenation of 4-nitrobenzonitrile, facilitated by CoCorrPPh₃@Vulcan-800. Reaction conditions: 4-nitrobenzonitrile (0.5 mmol), catalyst (0.5 mol%), H₂ (40 bar), MeOH (2 mL), 120 °C, 16 h, and *n*-hexadecane as the internal standard (18 mg).

Entry	Run	Conversion (%)
1	1	>99
2	2	90
3	3	59
4	4	49
5	5	44
6	6	40
7	7	39
8	8	37
9	9	36

3. Experimental

All chemicals were purchased from different commercial suppliers (Merck, Darmstadt, Germany; Fluorochem, Hadfield, UK; Acros Organics, Vienna, Austria; Alfa Aesar, Kandel, Germany; BLDPharm, Shanghai, China; VWR, Radnor, PA, USA; Roth, Karlsruhe, Germany; TCI, Oxford, UK; and Chem Lab, Zedelgem, Belgium) and used as received without further purification. The catalyzed hydrogenation reactions were carried out in a steel autoclave (Parr, Moline, IL, USA) (300 mL) that was pressurized with H₂ gas (5.0 purity, Linde Gas GmbH). Routine GC-MS analyses were carried out on a GC-MS QP-2020 (Shimadzu, Kyōto, Japan) device (He carrier gas, 5.0 purity, Linde Gas GmbH), whereas the HR-MS measurements were performed on a QTOF 6520 (Agilent, Santa Clara, CA, USA). The NMR data were collected on Avance III (Bruker, Billerica, MA, USA) spectrometers (300 MHz, 500 MHz) while the applied spectrometer frequencies of the various nuclei were as follows: 300 MHz (¹H NMR) and 75.5 MHz (¹³C{¹H} NMR) on the 300 MHz machine, whereas 470.5 MHz (¹⁹F NMR) on the 500 MHz spectrometer; the chemical shifts are listed in ppm on the δ -scale and axis calibration is based on the residual nondeuterated solvent signal that was used as a reference. The XPS data were acquired on a VG ESCALAB220iXL instrument (Thermo Fisher Scientific, Waltham, MA, USA, 1486.68 eV Al K α radiation). The scanning transmission electron microscopy (STEM) micrographs were conducted on a probe aberration-corrected JEM-ARM200F electron microscope (JEOL, Tokyo, Japan, CEOS corrector) equipped with a JED-2300 (JEOL) energy-dispersive X-ray spectrometer that has a silicon drift detector (dry SD60GV). A high-angle annular dark field (HAADF) and an annular bright field (ABF) detector were used for general imaging. The solid sample was deposited without any pretreatment on a holey, carbon supported Cu grid (mesh 300) and transferred to the microscope. For the CHN analyses, a Microanalyser TruSpec (Leco, Geleen, The Netherlands) machine was employed, whereas the metal content was determined via Atomic Absorption Spectroscopy using (PerkinElmer, Waltham, MA, USA) an AAS Analyst 300 device. Eventually, the TGA curves were recorded on a Pyris Series TGA4000 (PerkinElmer, Waltham, MA, USA) thermogravimetric analyzer.

3.1. Procedure for the Pyrolytic Synthesis of the Supported Cobalt-Corrole-Based Heterogeneous Catalyst

Initially, the soluble precursor complex **CoCorrPPh₃** (206 mg, 0.2 mmol) was dissolved in EtOH (30 mL), followed by a portioned addition of 1.00 g of the solid support (CeO₂, SiO₂, Al₂O₃, or Vulcan[®] XC 72 R) to this solution within a period of 30 min. The obtained suspension was then refluxed (6 h) and, after evaporation of the solvent under reduced pressure, the remaining solid was further dried in vacuo. Hereafter, the resultant **CoCorrPPh₃**-support composite was finely grinded using mortar and pestle (both made

of agate), upon which the formed powder was carefully pyrolyzed in an Austromat[®] 624 furnace at the required temperature (Ar atmosphere, 2 h). Thus, the obtained, full-fledged catalyst is referred to as CoCorrPPh₃@support-X, where X denotes the applied pyrolysis temperature (°C).

3.2. General Procedure for the Catalytic Hydrogenation Reactions

The catalyzed hydrogenation reactions were carried out in glass vials (4 mL), each of which was charged with solid CoCorrPPh₃@Vulcan-800 (12 mg, if not stated otherwise, i.e., 0.5 mol% based on a bulk Co content of 1.16% by weight), nitro compound (0.5 mmol), solvent (2 mL), as well as a magnetic stirring bar—in that order and without any protection from air. Each reaction vessel was sealed with a septum cap, which was then pierced with a steel canula. Hereafter, the vials were placed in a drilled Al plate that was transferred into the autoclave, upon which the latter was flushed with H₂ (3 × 40 bar) before being pressurized to the desired value. Afterwards, the autoclave was placed on a heating plate whereupon the stirring rate (1000 rpm) and the required temperature were adjusted. Upon completion of the reaction, the autoclave was allowed to reach room temperature, and, after that, the steel vessel was carefully de-pressurized. Subsequently, the catalyst was separated by centrifugation whereby the collected solid was washed five times with methanol. Eventually, the combined supernatants were evaporated to dryness under reduced pressure and further dried in vacuo.

Safety Statement concerning the Use of Pressurized Hydrogenation Gas

The pressurized H₂-containing steel bottle (200 bar, 50 L) was placed and lashed in a safety storage cabinet that is equipped with a tapping unit, whereby the gas cylinder was attached to a control panel that allowed for fine-tuning of the required H₂ pressure. The autoclave charging procedure was performed in a fume hood with an integrated sensor, which was wired to a magnetic valve. The latter promptly interrupts the gas feed in case of any H₂ leakage that might occur during the filling procedure. Moreover, optical and acoustic alerts are triggered whenever free flammable (and toxic) gas is detected inside the hood.

3.3. General Procedure for the Isolation of the Organic Ammonium Salts

The corresponding hydrochloride salts of the prepared amines (Section 3.2) were, if desired, obtained by the initial treatment of the crude product with etheric HCl (2 mL, 2 M in Et₂O). The formed precipitate was filtered off, washed with dichloromethane (DCM) (3 × 0.5 mL), and finally dried in vacuo.

4. Conclusions

We herein communicated the straightforward manufacture and characterization (XPS, EDX, and HAADF-STEM) of an immobilized cobalt-based catalyst that was prepared through pyrolytic synthesis of a Vulcan[®] XC 72 R-supported heteroleptic Co-corrole complex. The given functional solid was applied in the heterogeneous hydrogenation of a broad variety of nitroarenes to furnish the corresponding anilines, which were conveniently isolated as their hydrochloride salts. In addition, the introduced synthetic protocol provided excellent chemoselectivity under exceptionally low catalyst loadings (0.5 mol% per nitro group based on the bulk Co content) that were generally applied for the establishment of the product portfolio, irrespective of the complexity of the used substrates.

Since the reaction assembly is readily prepared under open-flask conditions without the need for time-consuming operating steps in containment systems (glovebox, -bags, etc.), this hydrogenation method is well-suited for the practically oriented synthetic chemist.

Finally, the fact that homoleptic metal corrole complexes still have vacant coordination sites allows for the deliberate introduction of foreign atoms into the catalyst matrix. This trait paves the way for the design of composite materials with tailor-made properties.

Supplementary Materials: The following supporting information can be downloaded at: <https://www.mdpi.com/article/10.3390/catal12010011/s1>, Effect of temperature and H₂ pressure, dependence on the reaction time, control experiments, Maitlis' hot filtration test, catalyst characterization (EA, XPS, EDX, and TGA), synthesis and characterization of CoCorrPPh₃, characterization of the isolated products (yield, ¹H NMR, ¹³C NMR, ¹⁹F NMR, HR-MS).

Author Contributions: Conceptualization: J.M. and C.T.; methodology: J.M. and C.T.; validation: J.M., M.H., T.B., and D.K.; formal analysis: J.M., M.H., D.K., T.B., N.R., and S.B.; investigation: J.M., M.H., D.K., T.B., N.R. and S.B.; writing—original draft preparation: J.M. and C.T.; writing—review and editing: C.T. and W.S.; visualization: J.M., M.H., D.K., N.R., and S.B.; supervision: C.T. and W.S.; funding acquisition: W.S. and C.T. All authors have read and agreed to the published version of the manuscript.

Funding: Open Access Funding by the Austrian Science Fund (FWF). Standalone Project P 32045 'Metalloporphyrin-Based Catalyst for Biomass Valorization'. For the purpose of open access, the author has applied a CC BY public copyright license to any Author Accepted Manuscript version arising from this submission.

Data Availability Statement: Not applicable.

Acknowledgments: We gratefully thank Marko Hapke from INCA for fruitful discussions and the generous support. Moreover, we are much obliged to Klaus Bretterbauer from the Institute of Chemical Technology of Organic Materials (CTO) at the JKU for carrying out TGA measurements on the pristine phosphine-ligated Co-corrolate, and finally Astrid Lehmann from the Leibniz Institute for Catalysis (LIKAT) in Rostock for providing the elemental analysis results.

Conflicts of Interest: The authors declare that they have no conflict of interest.

References

1. Béchamp, A. De l'action des protocels de fer sur la nitronaphtaline et la nitrobenzine. nouvelle méthode de formation des bases organiques artificielles de Zinin. *Ann. Chim. Phys.* **1854**, *42*, 186–196.
2. Downing, R.; Kunkeler, P.; van Bekkum, H. Catalytic syntheses of aromatic amines. *Catal. Today* **1997**, *37*, 121–136. [[CrossRef](#)]
3. Blaser, H.-U.; Steiner, H.; Studer, M. Selective Catalytic Hydrogenation of Functionalized Nitroarenes: An Update. *ChemCatChem* **2009**, *1*, 210–221. [[CrossRef](#)]
4. Orlandi, M.; Brenna, D.; Harms, R.; Jost, S.; Benaglia, M. Recent developments in the reduction of aromatic and aliphatic nitro compounds to amines. *Org. Process. Res. Dev.* **2018**, *22*, 430–445. [[CrossRef](#)]
5. Formenti, D.; Ferretti, F.; Scharnagl, F.; Beller, M. Reduction of Nitro Compounds Using 3d-Non-Noble Metal Catalysts. *Chem. Rev.* **2018**, *119*, 2611–2680. [[CrossRef](#)]
6. Corma, A.; González-Arellano, C.; Iglesias, M.; Sánchez, F. Gold complexes as catalysts: Chemoselective hydrogenation of nitroarenes. *Appl. Catal. A Gen.* **2009**, *356*, 99–102. [[CrossRef](#)]
7. Harsy, S.G. Homogeneous hydrogenation of nitroaliphatic compounds catalyzed by group VIII transition metal phosphine complexes. *Tetrahedron* **1990**, *46*, 7403–7412. [[CrossRef](#)]
8. Yu, Z.; Liao, S.; Xu, Y.; Yang, B.; Yu, D. Hydrogenation of nitroaromatics by polymer-anchored bimetallic palladium-ruthenium and palladium-platinum catalysts under mild conditions. *J. Mol. Catal. A Chem.* **1997**, *120*, 247–255. [[CrossRef](#)]
9. Xu, S.; Xi, X.; Shi, J.; Cao, S. A homogeneous catalyst made of poly(4-vinylpyridine-co-N-vinylpyrrolidone)-Pd(0) complex for hydrogenation of aromatic nitro compounds. *J. Mol. Catal. A Chem.* **2000**, *160*, 287–292. [[CrossRef](#)]
10. Zakhariev, A.; Ivanova, V.; Khidekel, M.L.; Chepaikin, E.G.; Shopov, D. Hydrogenation of aromatic nitro compounds in the presence of the platinum(II) complex of 1-phenylazo-2-naphthol in DMF. *React. Kinet. Catal. Lett.* **1978**, *8*, 195–201.
11. Chepaikin, E.G.; Ivanova, V.V.; Zakhariev, A.I.; Shopov, D.M. Homogeneous catalytic hydrogenation of aromatic nitrocompounds by complexes of the platinum group metal with dyes. The reaction of nitrobenzene with a complex of rhodium with the anion-radical of potassium indigodisulfonate. *J. Mol. Catal.* **1980**, *10*, 115–119. [[CrossRef](#)]
12. Knifton, J.F. Homogeneous catalyzed reduction of nitro compounds. IV. Selective and sequential hydrogenation of nitroaromatics. *J. Org. Chem.* **1976**, *41*, 1200–1206. [[CrossRef](#)]
13. Toti, A.; Frediani, P.; Salvini, A.; Rosi, L.; Giolli, C. Hydrogenation of single and multiple N–N or N–O bonds by Ru(II) catalysts in homogeneous phase. *J. Organomet. Chem.* **2005**, *690*, 3641–3651. [[CrossRef](#)]
14. Deshmukh, A.A.; Prashar, A.K.; Kinage, A.K.; Kumar, R.; Meijboom, R. Ru(II) Phenanthroline Complex As Catalyst for Chemoselective Hydrogenation of Nitro-Aryls in a Green Process. *Ind. Eng. Chem. Res.* **2010**, *49*, 12180–12184. [[CrossRef](#)]
15. Deshpande, R.M.; Mahajan, A.N.; Diwakar, M.M.; Ozarde, P.S.; Chaudhari, R.V. Chemoselective Hydrogenation of Substituted Nitroaromatics Using Novel Water-Soluble Iron Complex Catalysts. *J. Org. Chem.* **2004**, *69*, 4835–4838. [[CrossRef](#)] [[PubMed](#)]
16. Wienhöfer, G.; Baseda-Krüger, M.; Ziebart, C.; Westerhaus, F.A.; Baumann, W.; Jackstell, R.; Junge, K.; Beller, M. Hydrogenation of nitroarenes using defined iron–phosphine catalysts. *Chem. Commun.* **2013**, *49*, 9089–9091. [[CrossRef](#)] [[PubMed](#)]

17. Zubar, V.; Dewanji, A.; Rueping, M. Chemoselective Hydrogenation of Nitroarenes Using an Air-Stable Base-Metal Catalyst. *Org. Lett.* **2021**, *23*, 2742–2747. [[CrossRef](#)] [[PubMed](#)]
18. Timelthaler, D.; Schöfberger, W.; Topf, C. Selective and Additive-Free Hydrogenation of Nitroarenes Mediated by a DMSO-Tagged Molecular Cobalt Corrole Catalyst. *Eur. J. Org. Chem.* **2021**, *2021*, 2114–2120. [[CrossRef](#)]
19. Westerhaus, F.A.; Jagadeesh, R.V.; Wienhöfer, G.; Pohl, M.-M.; Radnik, J.; Surkus, A.-E.; Rabeah, J.; Junge, K.; Junge, H.; Nielsen, M.; et al. Heterogenized cobalt oxide catalysts for nitroarene reduction by pyrolysis of molecularly defined complexes. *Nat. Chem.* **2013**, *5*, 537–543. [[CrossRef](#)]
20. Jagadeesh, R.V.; Surkus, A.-E.; Junge, H.; Pohl, M.-M.; Radnik, J.; Rabeah, J.; Huan, H.; Schünemann, V.; Brückner, A.; Beller, M. Nanoscale Fe₂O₃-based catalysts for selective hydrogenation of nitroarenes to anilines. *Science* **2013**, *342*, 1073–1076. [[CrossRef](#)]
21. Formenti, D.; Topf, C.; Junge, K.; Ragaini, F.; Beller, M. Fe₂O₃/NGr@C- and Co-Co₃O₄/NGr@C-catalysed hydrogenation of nitroarenes under mild conditions. *Cat. Sci. Technol.* **2016**, *6*, 4473–4477. [[CrossRef](#)]
22. Jagadeesh, R.V.; Murugesan, K.; Alshammari, A.S.; Neumann, H.; Pohl, M.-M.; Radnik, J.; Beller, M. MOF-derived cobalt nanoparticles catalyze a general synthesis of amines. *Science* **2017**, *358*, 326–332. [[CrossRef](#)]
23. Zhou, P.; Jiang, L.; Wang, F.; Deng, K.; Lv, K.; Zhang, Z. High performance of a cobalt–nitrogen complex for the reduction and reductive coupling of nitro compounds into amines and their derivatives. *Sci. Adv.* **2017**, *3*, e1601945. [[CrossRef](#)]
24. Jiang, L.; Zhou, P.; Zhang, Z.; Jin, S.; Chi, Q. Synthesis of Secondary Amines from One-Pot Reductive Amination with Formic Acid as the Hydrogen Donor over an Acid-Resistant Cobalt Catalyst. *Ind. Eng. Chem. Res.* **2017**, *56*, 12556–12565. [[CrossRef](#)]
25. Jiang, L.; Zhou, P.; Zhang, Z.; Chi, Q.; Jin, S. Environmentally friendly synthesis of secondary amines via one-pot reductive amination over a heterogeneous Co–Nx catalyst. *New J. Chem.* **2017**, *41*, 11991–11997. [[CrossRef](#)]
26. Sahoo, B.; Formenti, D.; Topf, C.; Bachmann, S.; Scalone, M.; Junge, K.; Beller, M. Biomass-Derived Catalysts for Selective Hydrogenation of Nitroarenes. *ChemSusChem* **2017**, *10*, 3035–3039. [[CrossRef](#)] [[PubMed](#)]
27. Cui, X.; Liang, K.; Tian, M.; Zhu, Y.; Ma, J.; Dong, Z. Cobalt nanoparticles supported on N-doped mesoporous carbon as a highly efficient catalyst for the synthesis of aromatic amines. *J. Colloid Interface Sci.* **2017**, *501*, 231–240. [[CrossRef](#)] [[PubMed](#)]
28. Reddy, P.L.; Tripathi, M.; Arundhati, R.; Rawat, D.S. Chemoselective Hydrazine-mediated Transfer Hydrogenation of Nitroarenes by Co₃O₄ Nanoparticles Immobilized on an Al/Si-mixed Oxide Support. *Chem.–Asian J.* **2017**, *12*, 785–791. [[CrossRef](#)]
29. Stadler, L.; Homafar, M.; Hartl, A.; Najafshir, S.; Colombo, M.; Zboril, R.; Martin, P.; Gawande, M.B.; Zhi, J.; Reiser, O. Recyclable Magnetic Microporous Organic Polymer (MOP) Encapsulated with Palladium Nanoparticles and Co/C Nanobeads for Hydrogenation Reactions. *ACS Sustain. Chem. Eng.* **2018**, *7*, 2388–2399. [[CrossRef](#)]
30. Kim, D.Y.; Choi, T.J.; Gil Kim, J.; Chang, J.Y. A Cobalt Tandem Catalyst Supported on a Compressible Microporous Polymer Monolith. *ACS Omega* **2018**, *3*, 8745–8751. [[CrossRef](#)]
31. Mullangi, D.; Chakraborty, D.; Pradeep, A.; Koshti, V.; Vinod, C.P.; Panja, S.; Nair, S.; Vaidhyanathan, R. Highly stable COF-supported Co/Co(OH)₂ nanoparticles heterogeneous catalyst for reduction of nitrile/nitro compounds under mild conditions. *Small* **2018**, *14*, 1801233. [[CrossRef](#)] [[PubMed](#)]
32. Chen, C.; Li, X.; Deng, J.; Wang, Z.; Wang, Y. Shape Engineering of Biomass-Derived Nanoparticles from Hollow Spheres to Bowls through Solvent-Induced Buckling. *ChemSusChem* **2018**, *11*, 2540–2546. [[CrossRef](#)] [[PubMed](#)]
33. Sun, X.; Olivos-Suarez, A.I.; Osadchii, D.; Romero, M.J.V.; Kapteijn, F.; Gascon, J. Single cobalt sites in mesoporous N-doped carbon matrix for selective catalytic hydrogenation of nitroarenes. *J. Catal.* **2018**, *357*, 20–28. [[CrossRef](#)]
34. Xu, Y.; Long, J.; Zhao, W.; Li, H.; Yang, S. Efficient Transfer Hydrogenation of Nitro Compounds to Amines Enabled by Mesoporous N-Stabilized Co–Zn/C. *Front. Chem.* **2019**, *7*, 590. [[CrossRef](#)] [[PubMed](#)]
35. Dai, Y.; Jiang, C.; Xu, M.; Bian, B.; Lu, D.; Yang, Y. Cobalt in N-doped carbon matrix catalyst for chemoselective hydrogenation of nitroarenes. *Appl. Catal. A Gen.* **2019**, *580*, 158–166. [[CrossRef](#)]
36. Li, H.; Cao, C.; Liu, J.; Shi, Y.; Si, R.; Gu, L.; Song, W. Cobalt single atoms anchored on N-doped ultrathin carbon nanosheets for selective transfer hydrogenation of nitroarenes. *Sci. China Mater.* **2019**, *62*, 1306–1314. [[CrossRef](#)]
37. Bhattacharyya, S.; Samanta, D.; Roy, S.; Radhakantha, V.P.H.; Maji, T.K. In situ Stabilization of Au and Co Nanoparticles in a Redox-Active Conjugated Microporous Polymer Matrix: Facile Heterogeneous Catalysis and Electrocatalytic Oxygen Reduction Reaction Activity. *ACS Appl. Mater. Interfaces* **2019**, *11*, 5455–5461. [[CrossRef](#)]
38. Li, W.; Artz, J.; Broicher, C.; Junge, K.; Hartmann, H.; Besmehn, A.; Palkovits, R.; Beller, M. Superior activity and selectivity of heterogenized cobalt catalysts for hydrogenation of nitroarenes. *Catal. Sci. Technol.* **2018**, *9*, 157–162. [[CrossRef](#)]
39. Nanadegani, Z.S.; Nemati, F.; Elhampour, A.; Rangraz, Y. Cobalt oxide NPs immobilized on environmentally benign biological macromolecule-derived N-doped mesoporous carbon as an efficient catalyst for hydrogenation of nitroarenes. *J. Solid State Chem.* **2020**, *292*, 121645. [[CrossRef](#)]
40. Bustamante, T.M.; Campos, C.H.; Fraga, M.A.; Fierro, J.L.G.; Pecchi, G. Promotional effect of palladium in Co–SiO₂ core@shell nanocatalysts for selective liquid phase hydrogenation of chloronitroarenes. *J. Catal.* **2020**, *385*, 224–237. [[CrossRef](#)]
41. Cao, Y.; Liu, K.; Wu, C.; Zhang, H.; Zhang, Q. In situ-formed cobalt embedded into N-doped carbon as highly efficient and selective catalysts for the hydrogenation of halogenated nitrobenzenes under mild conditions. *Appl. Catal. A Gen.* **2020**, *592*. [[CrossRef](#)]
42. Minh, T.D.; Ncibi, M.C.; Certenais, M.; Viitala, M.; Sillanpää, M. Cobalt-lignosulfonate complex derived non-noble catalysts: Facile valorization for high-performance redox conversion of organic pollutants. *J. Clean. Prod.* **2020**, *253*, 120013. [[CrossRef](#)]

43. Liu, X.; Zhang, L.; Wang, J.; Shang, N.; Gao, S.; Wang, C.; Gao, Y. Transfer Hydrogenation of Nitroarenes Catalyzed by CoCu Anchored on Nitrogen-doped Porous Carbon. *Appl. Organomet. Chem.* **2020**, *34*, e5438. [\[CrossRef\]](#)
44. Gutiérrez-Tarriño, S.; Rojas-Buzo, S.; Lopes, C.W.; Agostini, G.; Calvino, J.J.; Corma, A.; Oña-Burgos, P. Cobalt nanoclusters coated with N-doped carbon for chemoselective nitroarene hydrogenation and tandem reactions in water. *Green Chem.* **2021**, *23*, 4490–4501. [\[CrossRef\]](#)
45. Huang, R.; Wang, Y.; Liu, X.; Zhou, P.; Jin, S.; Zhang, Z. Co–N_x catalyst: An effective catalyst for the transformation of nitro compounds into azo compounds. *React. Chem. Eng.* **2020**, *6*, 112–118. [\[CrossRef\]](#)
46. Formenti, D.; Ferretti, F.; Topf, C.; Surkus, A.-E.; Pohl, M.-M.; Radnik, J.; Schneider, M.; Junge, K.; Beller, M.; Ragaini, F. Co-based heterogeneous catalysts from well-defined α -diimine complexes: Discussing the role of nitrogen. *J. Catal.* **2017**, *351*, 79–89. [\[CrossRef\]](#)
47. Mohapatra, S.K.; Sonavane, S.U.; Jayaram, R.V.; Selvam, P. Heterogeneous catalytic transfer hydrogenation of aromatic nitro and carbonyl compounds over cobalt(II) substituted hexagonal mesoporous aluminophosphate molecular sieves. *Tetrahedron Lett.* **2002**, *43*, 8527–8529. [\[CrossRef\]](#)
48. Kulkarni, A.S.; Jayaram, R.V. Liquid phase catalytic transfer hydrogenation of aromatic nitro compounds on perovskites prepared by microwave irradiation. *Appl. Catal. A Gen.* **2003**, *252*, 225–230. [\[CrossRef\]](#)
49. Long, J.; Zhou, Y.; Li, Y. Transfer hydrogenation of unsaturated bonds in the absence of base additives catalyzed by a cobalt-based heterogeneous catalyst. *Chem. Commun.* **2014**, *51*, 2331–2334. [\[CrossRef\]](#) [\[PubMed\]](#)
50. Loos, P.; Alex, H.; Hassfeld, J.; Lovis, K.; Platzek, J.; Steinfeldt, N.; Hübner, S. Selective Hydrogenation of Halogenated Nitroaromatics to Haloanilines in Batch and Flow. *Org. Process. Res. Dev.* **2015**, *20*, 452–464. [\[CrossRef\]](#)
51. Zhao, T.-J.; Zhang, Y.-N.; Wang, K.-X.; Su, J.; Wei, X.; Li, X.-H. General transfer hydrogenation by activating ammonia-borane over cobalt nanoparticles. *RSC Adv.* **2015**, *5*, 102736–102740. [\[CrossRef\]](#)
52. Wei, Z.; Mao, S.; Sun, F.; Wang, J.; Mei, B.; Chen, Y.; Li, H.; Wang, Y. The synergic effects at the molecular level in CoS₂ for selective hydrogenation of nitroarenes. *Green Chem.* **2017**, *20*, 671–679. [\[CrossRef\]](#)
53. Chang, S.-T.; Wang, C.-H.; Du, H.-Y.; Hsu, H.-C.; Kang, C.-M.; Chen, C.-C.; Wu, J.C.S.; Yen, S.-C.; Huang, W.-F.; Chen, L.-C.; et al. Vitalizing fuel cells with vitamins: Pyrolyzed vitamin B12 as a non-precious catalyst for enhanced oxygen reduction reaction of polymer electrolyte fuel cells. *Energy Environ. Sci.* **2012**, *5*, 5305–5314. [\[CrossRef\]](#)
54. Dou, M.; He, D.; Shao, W.; Liu, H.; Wang, F.; Dai, L. Pyrolysis of Animal Bones with Vitamin B12: A Facile Route to Efficient Transition Metal-Nitrogen-Carbon (TM-N-C) Electrocatalysts for Oxygen Reduction. *Chem. Eur. J.* **2015**, *22*, 2896–2901. [\[CrossRef\]](#) [\[PubMed\]](#)
55. Liang, H.-W.; Brüller, S.; Dong, R.; Zhang, J.; Feng, X.; Müllen, K. Molecular metal–N_x centres in porous carbon for electrocatalytic hydrogen evolution. *Nat. Commun.* **2015**, *6*, 7992. [\[CrossRef\]](#) [\[PubMed\]](#)
56. Chen, B.; Shang, S.; Wang, L.; Zhang, Y.; Gao, S. Mesoporous carbon derived from vitamin B12: A high-performance bifunctional catalyst for imine formation. *Chem. Commun.* **2015**, *52*, 481–484. [\[CrossRef\]](#) [\[PubMed\]](#)
57. Ferraccioli, R.; Borovika, D.; Surkus, A.-E.; Kreyenschulte, C.; Topf, C.; Beller, M. Synthesis of cobalt nanoparticles by pyrolysis of vitamin B12: A non-noble-metal catalyst for efficient hydrogenation of nitriles. *Catal. Sci. Technol.* **2017**, *8*, 499–507. [\[CrossRef\]](#)
58. Koszarna, B.; Gryko, D.T. Efficient Synthesis of meso-Substituted Corroles in a H₂O–MeOH Mixture. *J. Org. Chem.* **2006**, *71*, 3707–3717. [\[CrossRef\]](#)
59. Jiang, X.; Shan, W.; Desbois, N.; Quesneau, V.; Brandès, S.; Van Caemelbecke, E.; Osterloh, W.R.; Blondeau-Patissier, V.; Gros, C.P.; Kadish, K.M. Mono-DMSO ligated cobalt nitrophenylcorroles: Electrochemical and spectral characterization. *New J. Chem.* **2018**, *42*, 8220–8229. [\[CrossRef\]](#)
60. Quesneau, V.; Shan, W.; Desbois, N.; Brandès, S.; Rousselin, Y.; Vanotti, M.; Blondeau-Patissier, V.; Naitana, M.; Fleurat-Lessard, P.; van Caemelbecke, E.; et al. Cobalt corroles with bis-ammonia or mono-DMSO axial ligands. Electrochemical, spectroscopic characterizations, and ligand binding properties. *Eur. J. Inorg. Chem.* **2018**, *38*, 4265–4277. [\[CrossRef\]](#)
61. Nardis, S.; Mandoj, F.; Stefanelli, M.; Paolesse, R. Metal complexes of corrole. *Coord. Chem. Rev.* **2019**, *388*, 360–405. [\[CrossRef\]](#)
62. Osterloh, W.R.; Quesneau, V.; Desbois, N.; Brandès, S.; Shan, W.; Blondeau-Patissier, V.; Paolesse, R.; Gros, C.P.; Kadish, K.M. Synthesis and the Effect of Anions on the Spectroscopy and Electrochemistry of Mono(dimethyl sulfoxide)-Ligated Cobalt Corroles. *Inorg. Chem.* **2019**, *59*, 595–611. [\[CrossRef\]](#)
63. Osterloh, W.R.; Desbois, N.; Quesneau, V.; Brandès, S.; Fleurat-Lessard, P.; Fang, Y.; Blondeau-Patissier, V.; Paolesse, R.; Gros, C.P.; Kadish, K.M. Old Dog, New Tricks: Innocent, Five-coordinate Cyanocobalt Corroles. *Inorg. Chem.* **2020**, *59*, 8562–8579. [\[CrossRef\]](#)
64. Li, X.; Lei, H.; Liu, J.; Zhao, X.; Ding, S.; Zhang, Z.; Tao, X.; Zhang, W.; Wang, W.; Zheng, X.; et al. Carbon Nanotubes with Cobalt Corroles for Hydrogen and Oxygen Evolution in pH 0–14 Solutions. *Angew. Chem. Int. Ed.* **2018**, *57*, 15070–15075. [\[CrossRef\]](#) [\[PubMed\]](#)
65. Kadish, K.M.; Frémond, L.; Ou, Z.; Shao, J.; Shi, C.; Anson, F.C.; Burdet, F.; Gros, C.P.; Barbe, A.J.-M.; Guillard, R. Cobalt(III) Corroles as Electrocatalysts for the Reduction of Dioxygen: Reactivity of a Monocorrole, Biscorroles, and Porphyrin–Corrole Dyads. *J. Am. Chem. Soc.* **2005**, *127*, 5625–5631. [\[CrossRef\]](#) [\[PubMed\]](#)
66. Schöffberger, W.; Faschinger, D.-I.F.; Chattopadhyay, S.; Bhakta, S.; Mondal, B.; Elemans, J.A.A.W.; Müllegger, S.; Tebi, M.S.S.; Koch, R.; Klappenberger, P.-D.D.F.; et al. A Bifunctional Electrocatalyst for Oxygen Evolution and Oxygen Reduction Reactions in Water. *Angew. Chem. Int. Ed.* **2016**, *55*, 2350–2355. [\[CrossRef\]](#)

67. Honig, H.C.; Krishnamurthy, C.B.; Borge-Durán, I.; Tasior, M.; Gryko, D.T.; Grinberg, I.; Elbaz, L. Structural and Physical Parameters Controlling the Oxygen Reduction Reaction Selectivity with Carboxylic Acid-Substituted Cobalt Corroles Incorporated in a Porous Carbon Support. *J. Phys. Chem. C* **2019**, *123*, 26351–26357. [\[CrossRef\]](#)
68. De, R.; Gonglach, S.; Paul, S.; Haas, M.; Sreejith, S.S.; Gerschel, P.; Apfel, U.-P.; Vuong, T.H.; Rabeah, J.; Roy, S.; et al. Electrocatalytic reduction of CO₂ to acetic acid by a molecular manganese corrole complex. *Angew. Chem. Int. Ed.* **2020**, *59*, 10527–10534. [\[CrossRef\]](#)
69. Gonglach, S.; Paul, S.; Haas, M.; Pillwein, F.; Sreejith, S.S.; Barman, S.; De, R.; Müllegger, S.; Gerschel, P.; Apfel, U.-P.; et al. Molecular cobalt corrole complex for the heterogeneous electrocatalytic reduction of carbon dioxide. *Nat. Commun.* **2019**, *10*, 3864. [\[CrossRef\]](#)
70. Barbe, J.-M.; Canard, G.; Brandès, S.; Jérôme, F.; Dubois, G.; Guillard, R. Metallocorroles as sensing components for gas sensors: Remarkable affinity and selectivity of cobalt(III) corroles for CO vs. O₂ and N₂. *Dalton Trans.* **2004**, *8*, 1208–1214. [\[CrossRef\]](#)
71. Yang, S.; Wo, Y.; Meyerhoff, M.E. Polymeric optical sensors for selective and sensitive nitrite detection using cobalt(III) corrole and rhodium(III) porphyrin as ionophores. *Anal. Chim. Acta* **2014**, *843*, 89–96. [\[CrossRef\]](#) [\[PubMed\]](#)
72. Yang, S.; Meyerhoff, M.E. Study of Cobalt(III) Corrole as the Neutral Ionophore for Nitrite and Nitrate Detection via Polymeric Membrane Electrodes. *Electroanalysis* **2013**, *25*, 2579–2585. [\[CrossRef\]](#) [\[PubMed\]](#)
73. Yang, S.; Peng, L.; Huang, P.; Wang, X.; Sun, Y.; Cao, C.; Song, W. Nitrogen, Phosphorus, and Sulfur Co-Doped Hollow Carbon Shell as Superior Metal-Free Catalyst for Selective Oxidation of Aromatic Alkanes. *Angew. Chem. Int. Ed.* **2016**, *55*, 4016–4020. [\[CrossRef\]](#) [\[PubMed\]](#)
74. Mahyari, M.; Nasrollah, G.J. Cobalt porphyrin supported on N and P co-doped graphene quantum dots/graphene as an efficient photocatalyst for aerobic oxidation of alcohols under visible-light irradiation. *Res. Chem. Intermed.* **2018**, *44*, 3641–3657. [\[CrossRef\]](#)
75. Gao, L.; Zhu, M.; Zhang, Z.; Cui, G. Cobalt-boron-oxide supported on N, P dual-doped carbon nanosheets as the trifunctional electrocatalyst and its application in rechargeable Zn-air battery and overall water-electrolysis. *Electrochim. Acta* **2019**, *327*, 134980. [\[CrossRef\]](#)
76. Liu, X.; Rao, L.; Yao, Y.; Chen, H. Phosphorus-doped carbon fibers as an efficient metal-free bifunctional catalyst for removing sulfamethoxazole and chromium (VI). *Chemosphere* **2019**, *246*, 125783. [\[CrossRef\]](#) [\[PubMed\]](#)
77. Zhang, H.; Clark, J.H.; Geng, T.; Zhang, H.; Cao, F. A carbon catalyst co-Doped with P and N for efficient and selective oxidation of 5-hydroxymethylfurfural into 2,5-diformylfuran. *ChemSusChem* **2020**, *14*, 456–466. [\[CrossRef\]](#)
78. Liang, D.; Lian, C.; Xu, Q.; Liu, M.; Liu, H.; Jiang, H.; Li, C. Interfacial charge polarization in Co₂P₂O₇@N, P co-doped carbon nanocages as Mott-Schottky electrocatalysts for accelerating oxygen evolution reaction. *Appl. Catal. B Environ.* **2019**, *268*, 118417. [\[CrossRef\]](#)
79. Zhang, X.; Chen, Y.; Chen, M.; Wang, B.; Yu, B.; Wang, X.; Zhang, W.; Yang, D. FeNi₃-modified Fe₂O₃/NiO/MoO₂ heterogeneous nanoparticles immobilized on N, P co-doped CNT as an efficient and stable electrocatalyst for water oxidation. *Nanoscale* **2020**, *12*, 3777–3786. [\[CrossRef\]](#)
80. Chen, L.; Ren, J.-T.; Yuan, Z.-Y. Atomic heterojunction-induced electron interaction in P-doped g-C₃N₄ nanosheets supported V-based nanocomposites for enhanced oxidative desulfurization. *Chem. Eng. J.* **2020**, *387*, 124164. [\[CrossRef\]](#)
81. Liu, Y.; Guan, X.; Huang, B.; Wei, Q.; Xie, Z. One-Step Synthesis of N, P-Codoped Carbon Nanosheets Encapsulated CoP Particles for Highly Efficient Oxygen Evolution Reaction. *Front. Chem.* **2020**, *7*. [\[CrossRef\]](#)
82. Wang, J.; Zeng, H.C. Hybrid OER Electrocatalyst Combining Mesoporous Hollow Spheres of N, P-Doped Carbon with Ultrafine Co₂NiO_x. *ACS Appl. Mater. Interfaces* **2020**, *12*, 50324–50332. [\[CrossRef\]](#) [\[PubMed\]](#)
83. Sun, K.; Li, D.; Lu, G.; Cai, C. Hydrogen Auto-transfer synthesis of quinoxalines from o-nitroanilines and biomass-based diols catalyzed by MOF-derived N, P co-doped cobalt catalysts. *ChemCatChem* **2020**, *13*, 373–381. [\[CrossRef\]](#)
84. Zhou, H.; Dong, H.; Wang, J.; Chen, Y. Cobalt anchored on porous N, P, S-doping core-shell with generating/activating dual reaction sites in heterogeneous electro-Fenton process. *Chem. Eng. J.* **2020**, *406*, 125990. [\[CrossRef\]](#)
85. Hu, M.; Zhu, J.; Zhou, W. Synthesis of oxygen vacancy-enriched N/P co-doped CoFe₂O₄ for high-efficient degradation of organic pollutant: Mechanistic insight into radical and nonradical evolution. *Environ. Pollut.* **2020**, *270*, 116092. [\[CrossRef\]](#)
86. Wang, C.; Wang, Z.; Wang, H.; Chi, Y.; Wang, M.; Cheng, D.; Zhang, J.; Wu, C.; Zhao, Z. Noble-metal-free Co@Co₂P/N-doped carbon nanotube polyhedron as an efficient catalyst for hydrogen generation from ammonia borane. *Int. J. Hydrog. Energy* **2021**, *46*, 9030–9039. [\[CrossRef\]](#)
87. Xing, C.; Zhang, Y.; Gao, Y.; Kang, Y.; Zhang, S. N, P co-doped microporous carbon as a metal-free catalyst for the selective oxidation of alcohols by air in water. *New J. Chem.* **2021**, *45*, 13877–13884. [\[CrossRef\]](#)
88. Zhang, Q.; Luo, F.; Long, X.; Yu, X.; Qu, K.; Yang, Z. N, P doped carbon nanotubes confined WN-Ni Mott-Schottky heterogeneous electrocatalyst for water splitting and rechargeable zinc-air batteries. *Appl. Catal. B Environ.* **2021**, *298*, 120511. [\[CrossRef\]](#)
89. Asif, A.H.; Rafique, N.; Hirani, R.A.K.; Wu, H.; Shi, L.; Sun, H. Heterogeneous activation of peroxymonosulfate by Co-doped Fe₂O₃ nanospheres for degradation of p-hydroxybenzoic acid. *J. Colloid Interface Sci.* **2021**, *604*, 390–401. [\[CrossRef\]](#)
90. Wang, X.; Huang, G.; Pan, Z.; Kang, S.; Ma, S.; Shen, P.K.; Zhu, J. One-pot synthesis of Mn₂P-Mn₂O₃ heterogeneous nanoparticles in a P, N-doped three-dimensional porous carbon framework as a highly efficient bifunctional electrocatalyst for overall water splitting. *Chem. Eng. J.* **2022**, *428*, 131190. [\[CrossRef\]](#)
91. Long, X.; Li, Z.; Gao, G.; Sun, P.; Wang, J.; Zhang, B.; Zhong, J.; Jiang, Z.; Li, F. Graphitic phosphorus coordinated single Fe atoms for hydrogenative transformations. *Nat. Commun.* **2020**, *11*, 4074. [\[CrossRef\]](#) [\[PubMed\]](#)

-
92. Fujita, S.; Yamaguchi, S.; Yamasaki, J.; Nakajima, K.; Yamazoe, S.; Mizugaki, T.; Mitsudome, T. Ni₂P Nanoalloy as an Air-Stable and Versatile Hydrogenation Catalyst in Water: P-Alloying Strategy for Designing Smart Catalysts. *Chem. Eur. J.* **2020**, *27*, 4439–4446. [[CrossRef](#)] [[PubMed](#)]
 93. Appleby, A.P.; Müller, F.; Carpy, A. Weed Control. In *Ullmann's Encyclopedia of Industrial Chemistry*; Wiley-VCH: Weinheim, Germany, 2003.
 94. Vogt, P.F.; Gerulis, J.J. Amines, Aromatic. In *Ullmann's Encyclopedia of Industrial Chemistry*; Wiley-VCH: Weinheim, Germany, 2000.